water

MDPI

Article

A Case Study on Settling Process in Inclined-Tube Gravity Sedimentation Tank for Drip Irrigation with the Yellow River Water

Keyuan Wang, Yunkai Li, Shumei Ren and Peiling Yang *

College of Water Resources and Civil Engineering, China Agricultural University, Beijing 100083, China; wangkeyuan@cau.edu.cn (K.W.); liyunkai@126.com (Y.L.); renshumei@126.com (S.R.)

* Correspondence: cau_yangpeiling@163.com; Tel.: +86-1381-177-8078

Received: 22 April 2020; Accepted: 8 June 2020; Published: 12 June 2020

Abstract: A sedimentation tank which can remove fine sediment with low cost and high efficiency is of great significance for the wide application of drip irrigation techniques with the Yellow River water. In this study, the settling process of an inclined-tube gravity sedimentation tank which has high removal efficiency for fine particles in practice was thoroughly investigated. The sediment concentration distribution in the tank was measured by an optical back-scattering turbidimeter. The sediment thickness at the tank bottom was also measured. In addition, the size grading of sediment deposited at different positions on the tank bottom and at different heights in the inclined tubes was also measured by a laser particle size analyzer. It was found that the removal efficiency of fine sediment was 64.7–69.7% in the inclined-tube gravity sedimentation tank, which was higher than that of the sedimentation tank without inclined tubes (with a sediment removal rate of 20.7–32%). The sediment was mainly deposited in the flow adjustment area and settlement area with inclined tubes. A suitable height for the inclined tubes was 70–90 cm. In addition, the water inlet, baffle, and overflow weir in the tank negatively affected the fine sediment settling in two experiment cases. The experimental results enhance our understanding of the sedimentation characteristics in the tank, and indicate the direction for the subsequent structural optimization of the tank.

Keywords: flow adjustment board; sediment concentration; sediment size grading; sediment thickness

1. Introduction

The Yellow River is the main irrigation water source of the Yellow River irrigation area, which covers an area of up to 5.18×10^6 hm^2. However, the high sediment concentration and the fine sediment of the Yellow River can easily block drip irrigation emitters [1–3]. A sedimentation tank is the most traditional and common equipment used to separate water and sediment in an environmentally friendly way and it plays a very important role in ensuring the safe operation of the drip irrigation system in the Yellow River irrigation area. Many studies have been carried out to improve the sediment removal efficiency in sedimentation tanks with conventional structure. Bajcar et al. [4,5] observed the effect of different water inlet and outlet positions in a tank on sediment deposition. Kreb [6] and Goula et al. [7] found that the movement speed of solid particles toward the tank bottom was accelerated and the amount of deposited sediment was increased when a flow control baffle was set at the inlet of the tank. Tamayol et al. [8] found that setting baffles at the swirl zone of a tank had the best effect on improving the sediment removal efficiency of the tank. Shahrokhi et al. [9] improved the settling efficiency of a tank by arranging baffles at suitable positions at the bottom of the tank. They also carried out research to obtain the proper arrangement angle and

quantity of baffles [10–12]. Csepai et al. [13] and Zong et al. [14] tested the improvement effect of an overflow weir on the settling efficiency of a tank. Hua et al. [15], Zhang et al. [16] and Wu et al. [17] proved that the flow kinetic energy dissipation and sediment settling was increased by setting a flow adjustment board in a tank. However, the sediment size in the Yellow River is extremely fine, and the volume of sediment with a particle size of less than 100 μm accounts for more than 90% of the total sediment volume. It is difficult for a tank with a traditional structure to effectively settle fine particles in the Yellow River.

Based on that, an inclined-tube gravity sedimentation tank which was mainly inspired by the ideal sedimentation theory was designed. Its most important feature was the installation of inclined tubes in the tank, which improved settling efficiency by reducing sedimentation distance and expanding the sedimentation area. At present, this kind of sedimentation tank has begun to be used in the Hetao irrigation district in Inner Mongolia, and it has worked very well in practice. A lot of experimental works have been conducted to demonstrate that tube settler had a better efficiency of sediment removal than traditional settler [18–24]. These studies used the influent and effluent water turbidity from the tubes as the main measurement for determining tube settler efficiency, but these studies all neglected the influence of the tank's structure on the tube settler efficiency. Scholars were also concerned about the appropriate layout parameters of inclined tubes. Sarkar et al. [25] used a dimensional analysis method to study the influence of inclined-plate layout parameters (spacing, length, roughness of the plate, etc.) on the settling efficiency. Salem et al. [26] proposed that the most important requirements for achieving effective separation in a tank with inclined plates were its hydraulic performance and the equal distribution of suspensions between settler channels. Kshitija Balwan et al. [27] conducted a pilot scale model installed at Ichalkaranji municipal water treatment plant, and found that the optimum removal was observed for the length 60 cm and inclination 45° of inclined tubes. Subramani and Thomas [28] conducted a laboratory scale tube settler model, and the results showed that the optimum inclination angle was 55° for settling the flocculent particles. Demir [29] proposed an empirical equation for the inclined-plate layout angle and the settling efficiency, while Abdolzadeh et al. [30] found that the angle of inclined tubes had no effect on settling velocity in high-speed or high-Reynolds-number flow. The above literature summary shows that there is no consensus on the appropriate layout parameters of inclined tubes. Therefore, it is necessary to study the layout parameters of inclined tubes for the Yellow River water treatment. Contrast with a large number of studies focusing on the part of inclined tubes in the inclined-tube sedimentation tank, there are a few research works about the observation of the settling process in the tank. Bandrowski et al. [31] tested the removal efficiency of different kinds of suspended solids in the tank. Xie et al. [32] and Ignjatovic [33] proposed the calculation formula of sediment removal efficiency in the tank by theoretical analysis. Based on this, research was carried out to observe the settling process of the whole inclined-tube gravity sedimentation tank in this paper; this will be beneficial to the improvement of the structure and the settling efficiency of the tank.

This study mainly focused on the following two aspects:

(1) To prove that the inclined-tube gravity sedimentation tank is more effective than the sedimentation tank with a conventional structure on the fine sediment removal.
(2) To investigate the settling process of the inclined-tube gravity sedimentation tank in detail, and provide a direction for subsequent structural optimization of the tanks.

2. Experimental Setup and Procedure

2.1. Configuration of Inclined-Tube Gravity Sedimentation Tank

The main structure of an inclined-tube gravity sedimentation tank includes the forebay, intake sluice, sedimentation tank, overflow weir, clear water tank and drainage hole. In the sedimentation tank, the water inlet, tank, flow adjustment board, baffle, inclined tubes and overflow weir are included (see Figures 1 and 2a). The working process of this tank is as follows: First, by opening the intake sluice, the water flows from the forebay into the tank. Then, the water flows through the flow adjustment board from the flow adjustment area (FAA, located between the water inlet and the flow

adjustment board) to the stable settlement area (SSA, located between the flow adjustment board and the baffle), making large particles deposit at the tank bottom firstly. Next, through the gap between the baffle and the tank bottom, the water flows down into the settlement area with inclined tubes (ISA, located between the baffle and the back wall of the tank, see Figure 2b). By shortening the sedimentation distance and increasing its area, fine particles can be deposited on the tube wall and slide down to the tank bottom. Finally, clean water overflows from the overflow weir and flows into the clean water tank through the filter screen. The sediment on the tank bottom can be washed away by opening the drainage hole.

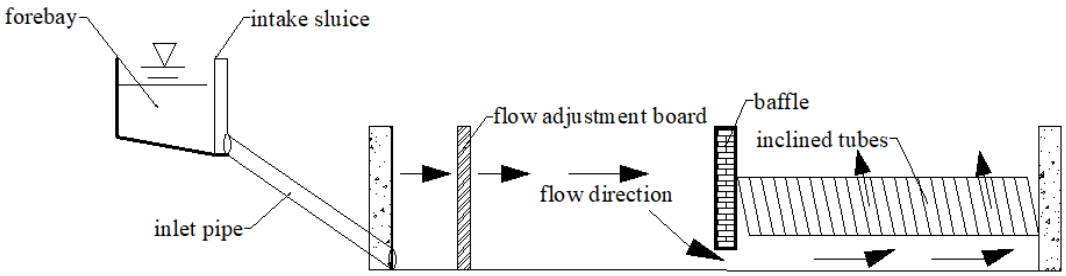

(**a**)

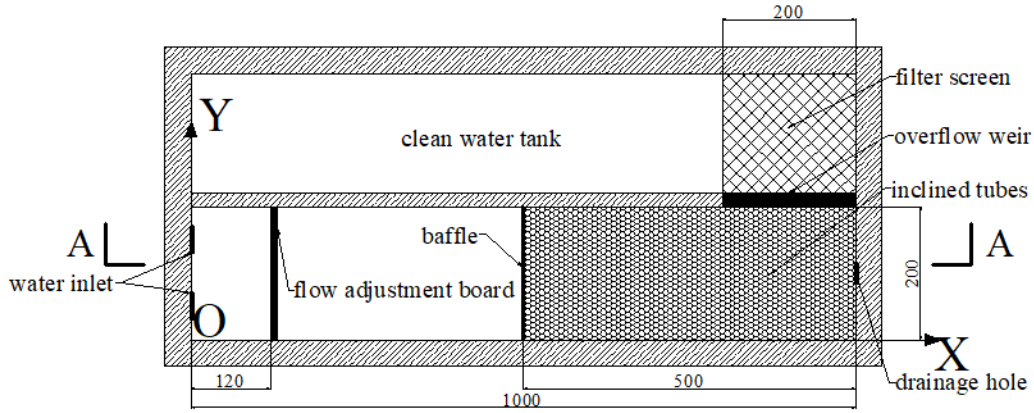

(**b**)

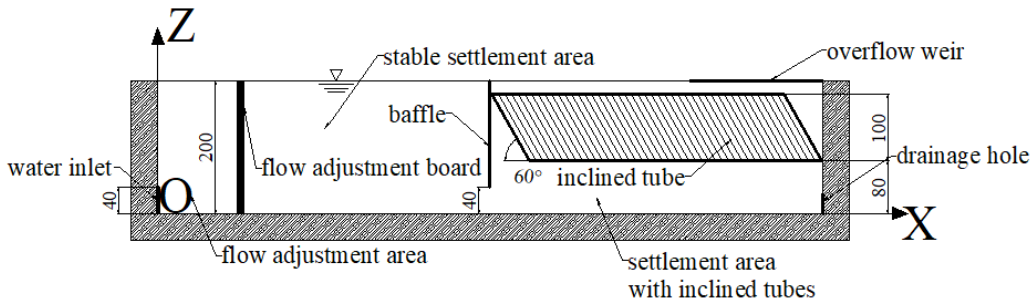

(**c**)

Figure 1. Schematic diagram of the inclined-tube gravity sedimentation tank: (**a**) flow direction in the inclined-tube gravity sedimentation tank, (**b**) vertical view of the inclined-tube gravity sedimentation tank, and (**c**) cross-sectional view of A-A of the inclined-tube gravity sedimentation tank (all the dimensions are in centimeters).

(**a**) (**b**)

Figure 2. Photographs of the inclined-tube gravity sedimentation tank: (**a**) full view of the inclined-tube gravity sedimentation tank, (**b**) detailed view of inclined tubes.

The most significant feature of the inclined-tube gravity sedimentation tank was that the inclined tubes were installed in the latter part of the tank, so the latter part of the tank was divided into two parts which were named SSA and ISA in this study. The main function of the SSA was to make the flow velocity distribution uniform and settle large particles, and the ISA mainly depended on the function that the inclined tubes could reduce the settling distance and increase the settling area to improve the settling efficiency of fine sediment. In contrast to the inclined-tube gravity sedimentation tank, the latter part of the conventionally structured sedimentation tank was a whole part which was just like the SSA with increased length, so the water flowed through this part straightly and overflows from the overflow weir. The sedimentation tank with conventional structure may be effective for settling large sediment, but the effect for settling fine sediment was very limited.

2.2. Experiment Establishment

In this part, two experimental cases are introduced.

2.2.1. Case 1

The experiment was conducted at the experiment station of China Agricultural University in the Hetao irrigation district, Inner Mongolia. A counterpart sedimentation tank with a design flow of 60 m^3/h, a length of 10 m, height of 2.2 m, and an operating water depth of 2 m, was established in the station. A flow adjustment board was installed 1.2 m away from the front wall of the tank in order to make the flow smooth and steady. The hole of the board was designed to be gradually larger from the bottom to the top and from the middle to the sides, and the holes on two sides were symmetrical (see Figure 3). Inclined tubes were installed at the latter part of the tank in order to ensure better sedimentation performance for the fine particles. The diameter of the hexagonal-prism inclined tubes was 50 mm and the vertical height of the tube was 1 m. There was a 60° angle between the tube and the horizontal plane. The laying area of the tubes was 10 m^2. The height between the bottom of the tubes and that of the tank was 0.8 m. A baffle was designed in front of the tubes to ensure that the water flowed into the bottom of the tubes through the gap (with a height of 0.4 m) between the baffle and the bottom of the tank. The overflow weir with a length of 2 m was set at the rear of the tank. In this study, the wall at the right side along the flow was called the right wall and the opposite one was called the left wall.

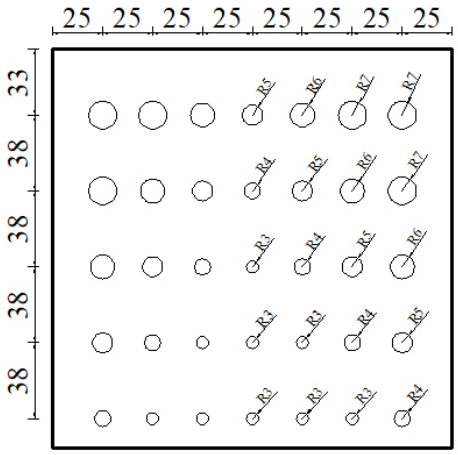

Figure 3. Schematic diagram of the flow adjustment board (all the dimensions are in centimeters).

2.2.2. Case 2

In order to compare the settling efficiency of an inclined-tube gravity sedimentation tank with that of a conventionally structured sedimentation tank, an additional experiment case was conducted on the inclined-tube gravity sedimentation tank while the inclined tubes were not installed in the tank.

The experimental water came from the Yellow River trunk canal next to the experimental station. Due to the fluctuation of sediment concentration in the trunk canal during the experiment, an appropriate amount of riverbed sediment was added to the forebay to ensure a constant sediment concentration of 3–3.5 kg/m^3 during the experiment.

A 3D coordinate axis was used to clearly express the positional information in the tank, where the x, y, and z axes denoted the flow direction (longitudinal), direction from the right wall to the left wall (transverse), and that from the bottom to the top of the tank (vertical). The origin of coordinates was represented by O (see Figure 1b,c).

2.3. Measurement

The sediment concentration at different locations in the sedimentation tank was measured in two experiment cases, while the sediment thickness, size grading of sediment deposited at the tank bottom and that at the inclined-tube walls were only measured in case 1. In order to verify the settling efficiency of the inclined-tube gravity sedimentation tank, the sediment concentration and size grading in the test water source were measured once a week during the experiment.

2.3.1. Measurement Locations

Sediment concentration measurement was carried out at 19 longitudinal sections (named sections 1–19) from upstream to downstream over the range x = 20–980 cm. The longitudinal spacing between adjacent sections was 60 cm. An additional section was set up at a distance of 20 cm in front of the flow adjustment board and the baffle, separately (see Figure 4a). The details of the measurement locations are illustrated in Figure 4b, where 36 sediment concentration samples were collected at each section. The measurement points are represented by the symbol "+". Height in the range of 0.8–1.8 m was occupied by inclined tubes in the ISA in case 1, so there were only two top-layer measurement points of sediment concentration below the free surface measured in the ISA. In case 2, the sediment concentration of all measurement locations in the ISA was measured.

Sediment thickness measurement at the tank bottom was also carried out at all sections. The measurement locations are presented in Figure 4b and are represented by the symbol "○".

The sediment size grading measurement locations are as follows. The measurement locations at the tank bottom are illustrated in Figure 4b, represented by red "×" symbols. The locations were measured at all sections. The measurement locations of inclined tubes are shown in Figure 4c. There

were eight inclined tubes measured in total, and they were divided into two rows along the x direction. Two rows of inclined tubes were each 40 cm away from the side walls. The four inclined tubes close to the left wall of the tank were named L1–L4 along the x direction. The other four inclined tubes close to the right wall were named R1–R4 along the x direction. In every measured tube, five locations of sediment were measured, which were marked as I–V from the bottom to the top of the inclined tubes.

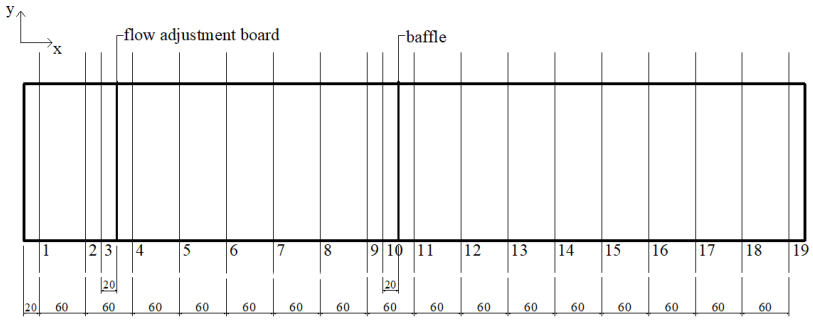

(**a**)

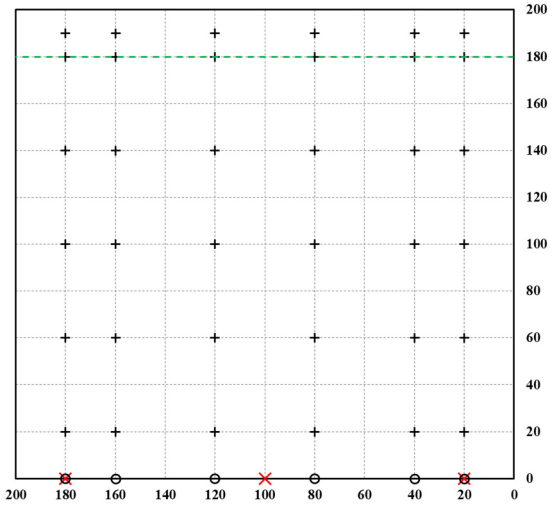

(**b**)

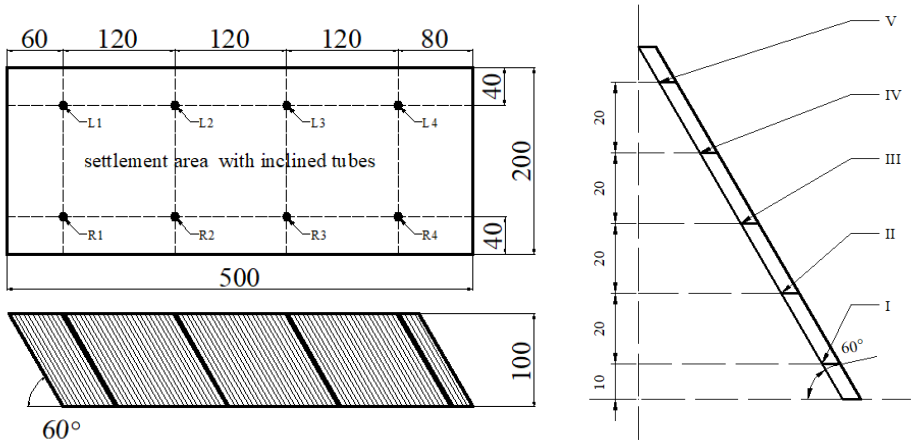

(**c**)

Figure 4. Measurement locations: (**a**) locations of measurement sections, (**b**) measurement locations arrangement in each section, and (**c**) measurement locations of inclined tubes (all the dimensions are in centimeters).

2.3.2. Measurement Methods

An optical back-scattering turbidimeter (OBS3+) was used for the sediment concentration measurement. It was fixed on a platform which could freely move along the tank longitudinally, transversely, and vertically, so it could reach every measurement location in the tank. The quantity of suspended sediment was acquired by receiving the scattered light of infrared radiation. Measurement was repeated three times at every measurement location, and the average value was taken as the measurement result to ensure measurement accuracy. The correlativity between the turbidity and concentration of the suspended sediment was established as follows. The measurement accuracy was ±4% ± 10 mg/L:

$$\beta = 3.5344 \times 10^{-5}\alpha^2 + 0.6975\alpha - 27.107 \quad (1)$$

$$\gamma = 3 \times 10^{-7}\beta^2 + 0.0011\beta + 0.1228 \quad (2)$$

where α refers the value measured by the OBS3+, β refers the turbidity value, and γ refers the sediment concentration value.

A laser particle size analyzer (Mastersizer 3000) was used to measure the size grading of deposited sediment. The grading data were acquired by receiving and measuring the energy distribution of the scattered light. The particle size measurement range of the Mastersizer 3000 was 0.01–3500 μm, and the measurement error was less than 1%. In order to ensure measurement accuracy, each sample was measured five times repeatedly, and the average value was taken as the measurement result. The sampling method of sediment samples was as follows: when the experiment case ended and the water in the tank was drained, the inclined tubes in the tank were taken out firstly, then deposited sediment on the measured tubes wall (shown in Figure 4c) was sampled separately according to different heights. Then, sediment samples at different measurement locations on the tank bottom were collected, and sediment samples were finally taken back to the laboratory for measurement. The sediment at different measurement locations was dried and then screened for 2 mm to remove impurities such as grass roots in sediment samples. Screened soil samples (0.2 g) at each position would be tested by following the operation steps of the instrument. In fact, actual particles (especially solid particles) are not usually spherical. In order to describe the size of irregularly shaped particles by particle size, the concept of equivalent diameter was introduced in the particle size measurement. In this experiment, particle size measured by the laser method was called the equivalent volume diameter, that is, the diameter of a sphere, the volume of which was equal to the volume of the particle. The particle diameter was automatically calculated by the software associated with the particle size analyzer.

The sediment thickness at the tank bottom was directly measured by a ruler when the experiment case ended and the water in the tank was drained.

2.3.3. Calculation Method

The surface measurement points in the ISA of section y = 180 cm is the closest to the overflow weir, so the sediment concentration in this area is close to that in the overflow. In this study, the average sediment concentration of these measurement points was regarded as the sediment concentration of overflow. Therefore, the sediment removal rate could be calculated by the following formula.

$$R_s = \frac{C_{tw} - C_{mp}}{C_{tw}} \quad (3)$$

where R_s refers to the sediment removal rate, C_{tw} refers to the sediment concentration of the test water source, and C_{mp} refers to the average sediment concentration of the surface measurement points in the ISA of section y = 180 cm.

3. Result and Analysis

3.1. Sediment Concentration Distribution

3.1.1. Case 1

The distribution of sediment concentration at different locations in the sedimentation tank is shown in Figure 5. Six y sections of y = 20, 40, 80, 120, 160 and 180 cm were analyzed in the plots. The sediment concentration of each section showed the same trend along the x direction. The concentration at the same height of the same y section gradually decreased along the x direction and finally reached about 1 kg/m^3 when flowing through the overflow weir.

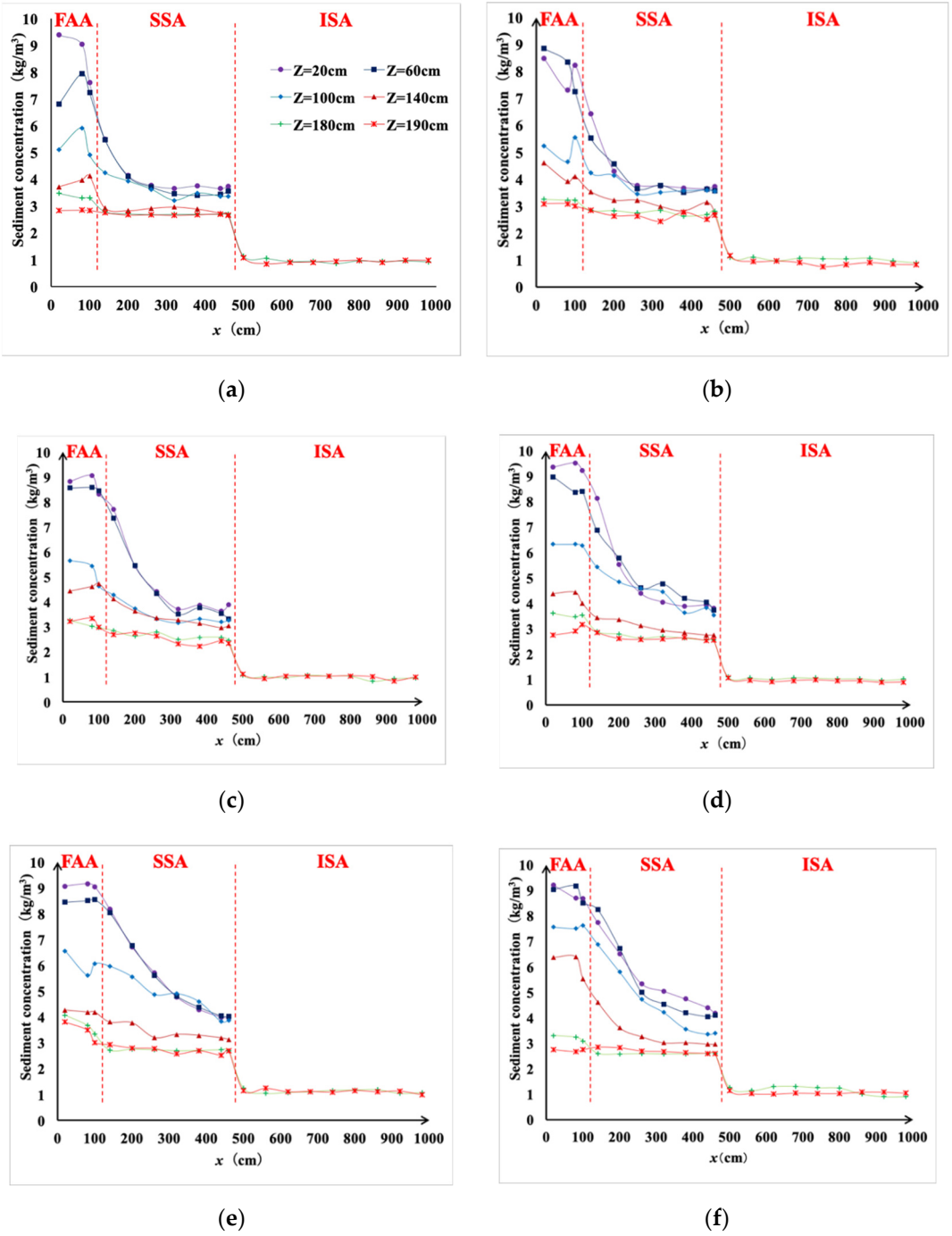

Figure 5. Distribution of sediment concentration at different measurement locations (case 1): (**a**) section of y = 20 cm, (**b**) section of y = 40 cm, (**c**) section of y = 80 cm, (**d**) section of y = 120 cm, (**e**) section of y = 160 cm, and (**f**) section of y = 180 cm.

In the FAA, the sediment concentration at the lower part of the tank (z = 20 and 60 cm) was large (8–10 kg/m^3), in the middle (z = 100 and 140 cm) it was lower than at the bottom (4–7 kg/m^3), and the concentration on the surface (z = 180 and 190 cm) was similar to that of the water source (3–4 kg/m^3). The sediment concentration in the middle and lower parts of the FAA was larger than that of the water source. This was caused by a large amount of sediment settling down at the tank bottom of the FAA in a long running time. With a large flow velocity, the flow from the water inlet washed away the sediment deposited on the bottom, and the sediment was turbulently diffused upward with the flow in the FAA.

In the SSA, the distribution of sediment concentration along the x direction was different at different heights. The concentration at the lower part (z = 20 and 60 cm) rapidly decreased in the front part (x = 120–300 cm) of the SSA, and in the latter part it continued to decrease but at a slower rate. Because the flow velocity decreased after passing through the flow adjustment board, large-sized sediment particles among the re-suspended sediment from the FAA bottom quickly settled to the tank bottom again. However, the settling velocity of fine sediment was small, leading to a slowdown decreased rate of the sediment concentration in the latter part of the SSA. The sediment concentration in the middle flow (z = 100 and 140 cm) slowly decreased in the SSA as a result of the sediment particles in the middle flow being smaller than those at the lower part. The variation curve of sediment concentration in the upper flow (z = 180 and 190 cm) was smooth in the SSA, which was caused by the fact that the sediment particles suspended in the upper flow were very small; therefore, the effect of flow turbulence on sediment settling was obvious.

In the ISA, only the sediment concentration in the upper part was measured. Compared with the concentration of the upper part of the end of the SSA, that of the upper part of the ISA was significantly decreased, from 2.5 down to 1 kg/m^3. The sediment concentration curve of the upper layer of the ISA was smoothly distributed along the x direction, indicating that the settling efficiency of different locations in the ISA was similar. The sediment concentration at a height of z = 180 cm was slightly larger than z = 190 cm. Among different y sections, the concentration of y = 180 cm was greater than other sections because that section was the closest to the overflow weir, and the overflow suction affected the flow pattern in the area, resulting in an increase in sediment concentration.

3.1.2. Case 2

Similar to the case 1, the distribution of sediment concentration at different locations in the tank of six y sections of y = 20, 40, 80, 120, 160 and 180 cm was also analyzed (see Figure 6). The sediment concentration of each section showed the same trend along the x direction.

In the FAA and the SSA, the sediment concentration distribution of case 2 is similar to that of case 1. In case 2, inclined tubes were not installed in the tank, so the sediment concentration distribution in the middle and lower part of the ISA was obtained. ① In the lower part of the ISA: The flow velocity became large when the water in the SSA flowed to the ISA from the gap between the baffle and the bottom of the tank, washing away the sediment that settled in the front section of the ISA. The sediment concentration of lower flow increased significantly in the front end of the ISA, and then decreased along the x direction, while only slightly increased at the end of the ISA, which was caused by the swirling flow in the triangle area formed by the tank bottom and the back wall. ② In the middle part of the ISA: Sediment concentration decreased slowly along the x direction. ③ In the upper part of the ISA: Sediment concentration almost did not decrease along the x direction, which indicated that it was difficult to remove the fine sediment in the Yellow River water only by prolonging the length of the sedimentation tank.

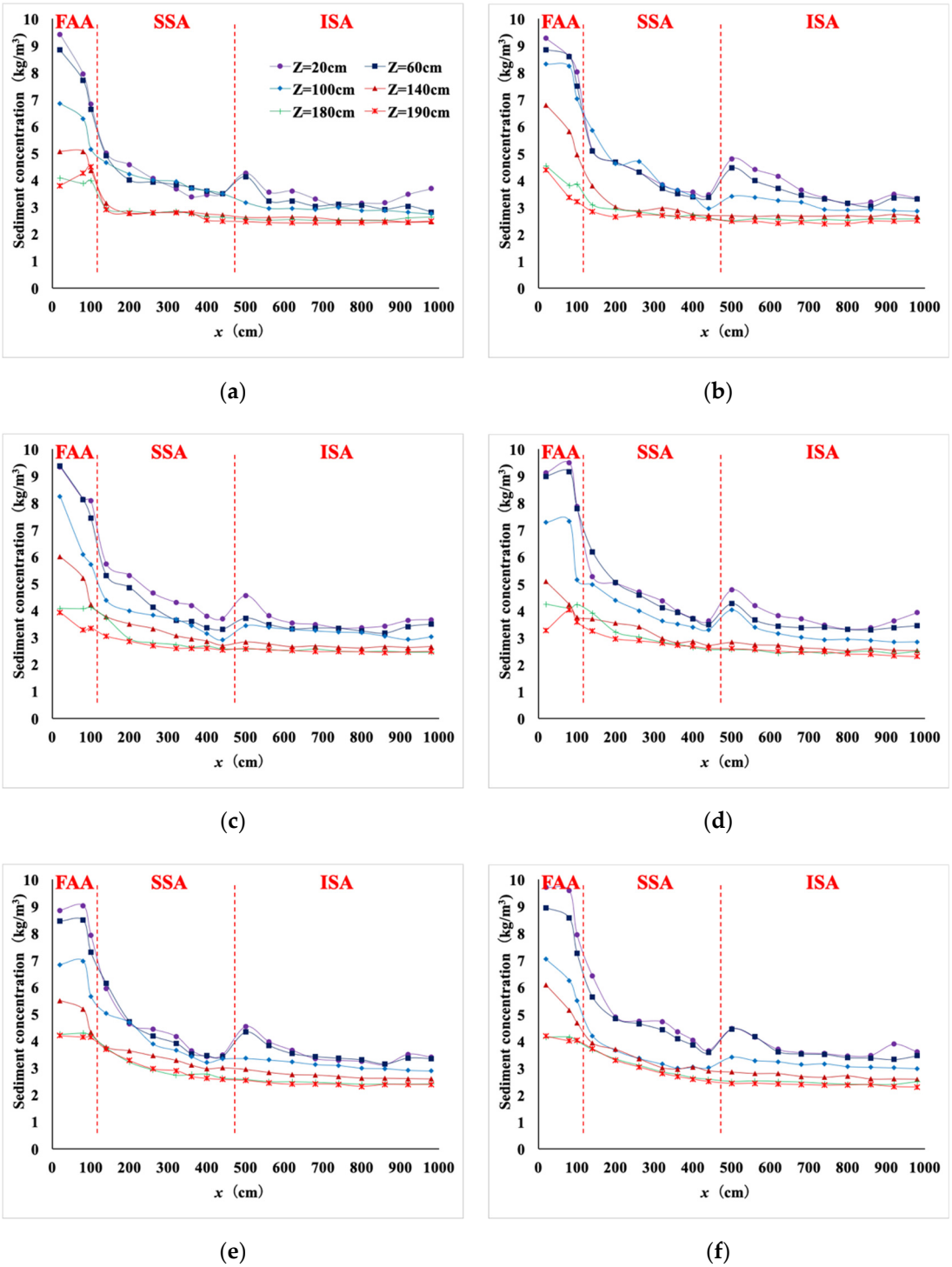

Figure 6. Distribution of sediment concentration at different measurement locations (case 2): (**a**) section of y = 20 cm, (**b**) section of y = 40 cm, (**c**) section of y = 80 cm, (**d**) section of y = 120 cm, (**e**) section of y = 160 cm, and (**f**) section of y = 180 cm.

The sediment removal rates of the two cases were obtained (see Table 1) according to the calculation of the test water source's sediment concentration and that of the surface measurement point in the ISA of section y = 180 cm.

Table 1. The sediment removal rate of two cases.

Case	C_{tw}	C_{mp}	R_s
Case 1	3–3.5 kg/m^3	1.06 kg/m^3	64.7%-69.7%
Case 2	3–3.5 kg/m^3	2.38 kg/m^3	20.7%-32%

The sediment removal rate of case 1 was 64.7%-69.7%, which was significantly higher than that of case 2. Sediment concentration almost did not decrease along the x direction in the ISA when inclined tubes were not installed in the tank. This showed that the inclined tubes had a great effect on the removal of fine sediment, and the inclined-tube gravity sedimentation tank had great advantages over the sedimentation tank with a conventional structure in terms of the removal of fine sediment.

3.2. Sediment Thickness at the Bottom of the Tank

The sediment thickness of six y sections of y = 20, 40, 80, 120, 160 and 180 cm and the average value of the six sections of sediment deposition thickness along the x direction are shown in Figure 7. The sediment thickness at the bottom of the tank was large at both ends and small in the middle.

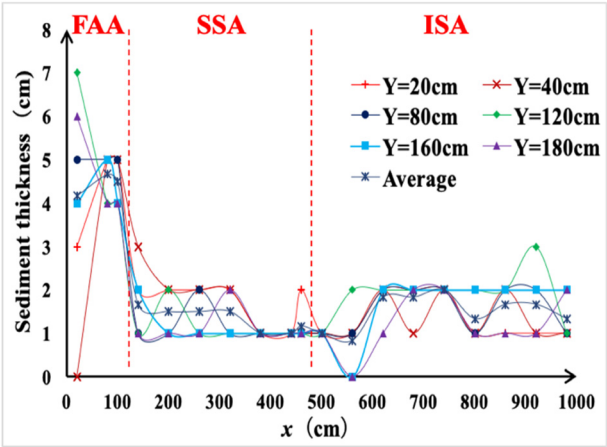

Figure 7. Sediment thickness of different sections at the bottom of the tank.

In the FAA, the thickness was large, up to 4–8 cm. During the experiment, sediment was added into the test water source to ensure that the sediment concentration was maintained at 3–3.5 kg/m^3. The added sediment was easily deposited at the bottom of the FAA and the large particles in the flow also settled in the FAA. Therefore, the sediment thickness in this area was significantly larger than that in other areas. In y = 20 and 40 cm sections, the sediment thickness was small at the location of x = 20 cm, which was caused by the high rate of flow from the water inlet washing away the sediment.

In the SSA, the thickness in the front part (x = 120–320 cm) was 2 cm and that in the latter part (x = 320–480 cm) was 1 cm, which was identical to the variation of sediment concentration in the tank's lower layer of case 1. This was caused by the large-sized particles settling in the front part of the SSA, while the small particles settled slowly in the latter part.

As for the ISA, the sediment thickness at the bottom of the tank was small just in the front part (x = 480–560 cm), while it was large in other parts (x = 560–980 cm). This was also due to the increase in the flow velocity near the baffle, washing away the sediment that settled in the front section of the ISA. Then, the flow with sediment moved up into the inclined tubes. The fine sediment in the flow easily settled on the tube walls, and then slid down to the bottom of the tank, so the sediment thickness became large in the latter part of the ISA.

At the same time, the variation of the sediment thickness in different y sections along the x direction was analyzed. It was found that the thickness of the y = 20 and 180 cm sections in the SSA and the ISA was smaller than that of other sections, indicating that a number of swirls were formed

at the corner between the side wall and the bottom of the tank. As a result, the sediment in this area was washed away by the flow.

3.3. Sediment Size Grading at Different Locations in the Tank

During the experiment, the sediment size grading in the test water was measured once a week. Most of the sediment particle size was less than 100 μm (see Figure 8). The sediment size grading of test water was similar to that of the Yellow River.

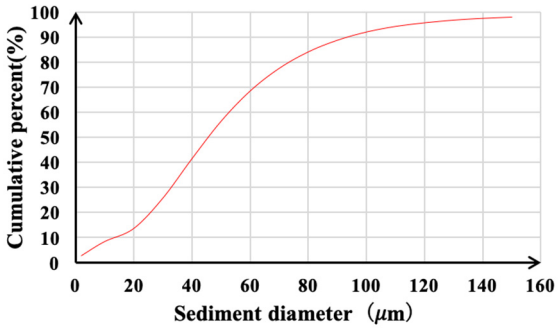

Figure 8. Percentage graph of sediment particle size accumulation of test water.

3.3.1. Sediment Size Grading at Different Locations on the Tank Bottom

The distribution curve of the sediment size grading along the x direction when y = 20, 100 and 180 cm is shown in Figure 9. Nine characteristic particle sizes of *d10*, *d20*, *d30*, *d40*, *d50*, *d60*, *d70*, *d80* and *d90* were analyzed. The variation trends of the sediment size grading in the three y sections were similar.

In the FAA, except for the particle size of *d90* being different when y = 100 cm, all characteristic particle sizes changes were distributed as a "crest" in all three y sections; i.e., the particle size was large at x = 80 cm, while it was small at x = 20 and 100 cm. Meanwhile, the characteristic particle sizes in this area were significantly larger than that of the test water source. It also verified the inference above, namely, that the large-sized sediment with poor mobility of the test water source settled at the bottom in the FAA. The sediment size grading at x = 100 cm was larger than that at x = 20 cm as a result of the flow velocity at the water inlet being large. The flow stroke on the flow adjustment board, then formed a vortex in the corner between the board and the bottom of the tank, and washed away the sediment at the bottom, in which the small-sized particles were re-suspended in the flow.

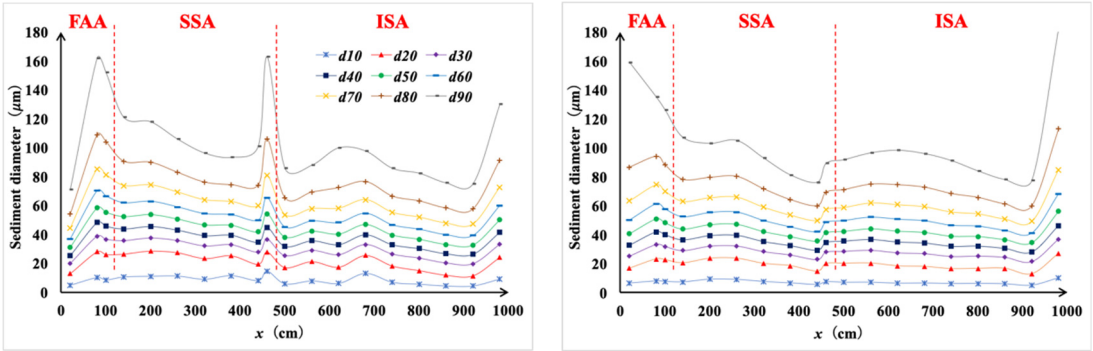

(**a**) (**b**)

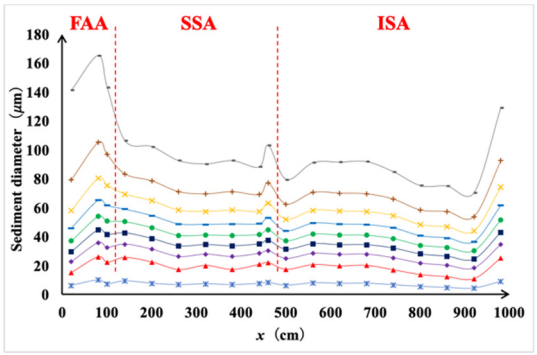

(**c**)

Figure 9. Sediment size grading along the x direction at the tank bottom: (**a**) section of y = 20 cm, (**b**) section of y = 100 cm, and (**c**) section of y = 180 cm.

In the SSA, the distribution of sediment size grading in each y section was completely consistent. Each characteristic particle size decreased along the x direction; it decreased fast in the front part (x = 120–320 cm) but slowly in the latter part (x = 320–440 cm), and it increased significantly only at the end (x = 440–460 cm). Because when the water flowed into the SSA, the velocity distribution tended to be uniform. In the front part, the large sediment quickly settled to the bottom of the tank, while in the latter part, the sediment were small, leading to slow settling. At the end, the characteristic particle sizes increased significantly as a result of the increase in the flow velocity near the baffle. The fine sediment at the bottom of the tank was washed away by the flow and re-suspended.

In the ISA, the characteristic particle sizes increased in the front part (x = 500–680 cm), while it decreased in the latter part (x = 680–920 cm). At the end (x = 920–980 cm), it increased significantly. Due to the fact that the fine sediment at the bottom of the tank in the end of the SSA was washed away by the high-speed flow and moved to the bottom in the front of the ISA, the characteristic particle sizes in this area were smaller. The latter part was not affected by the high-speed flow at the end of the SSA. The fine sediment in the flow was quickly deposited on the inclined-tube walls and slid to the tank bottom. The sediment particle size in the flow gradually decreased along the x direction, so the characteristic particle sizes in the latter part of the ISA gradually decreased, and that at the end increased significantly, which was caused by the vortex at the corner formed by the bottom and the back wall of the tank, washing away the sediment here and re-suspending the fine sediment into the flow.

3.3.2. Sediment Size Grading at Different Locations in the Inclined Tubes

Figure 10 shows the sediment size grading distribution of the inclined tubes at different locations and heights. According to the different locations of the inclined tubes in the sedimentation tank, eight parts of L1–L4 and R1–R4 were analyzed in plots. In all measured tubes, the characteristic particle sizes at heights I (10 cm), II (30 cm), and III (50 cm) were significantly different, while the differences of those at heights IV (70 cm) and V (90 cm) were not obvious.

L1, L2, R1 and R2 were in the front part of the ISA. In each tube, the characteristic particle sizes at heights I (10 cm), II (30 cm) and III (50 cm) were significantly larger than those at heights IV (70 cm) and V (90 cm). On the one hand, the sediment at the bottom in the end of the SSA was washed away by the high-speed water, re-suspended in the lower flow of the ISA, and entered with the flow into the inclined tubes in the front part of the ISA. On the other hand, the sediment particle size gradually decreased along the x direction, so most large particles entered into the tubes in the front part of the ISA.

L3, L4, R3 and R4 were in the latter part of the ISA. The sediment particle size in the lower part of the flow was small, so in each tube, the differences between the characteristic particle sizes at different heights were small. The characteristic particle sizes of L3 and L4 were slightly larger than

those at the same height of R3 and R4. This could be attributed to the overflow suction of the overflow weir having an effect on the steady flow in the inclined tubes.

At the same time, the characteristic particle sizes were not significantly different between the heights IV (70 cm) and V (90 cm) in all measured tubes, indicating that the effective vertical working height of the inclined tubes should be 70–90 cm. The sediment particle size of *d90* at the outlet of the measured tubes was about 40 μm, which was significantly smaller than 95 μm, the particle size of *d90* in the test water source, indicating that the inclined-tube gravity sedimentation tank performed well at removing fine sediment.

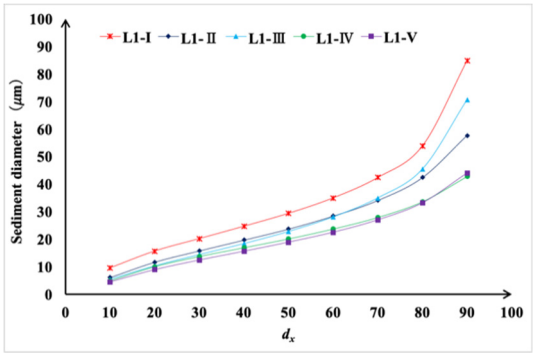

(**a**)

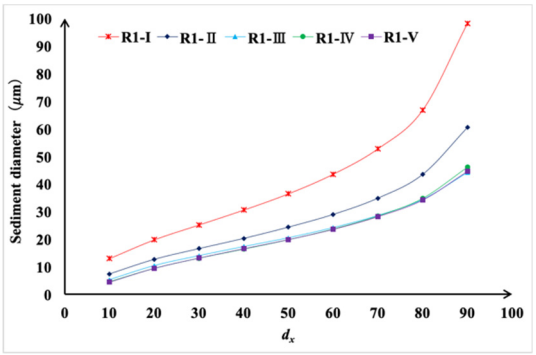

(**b**)

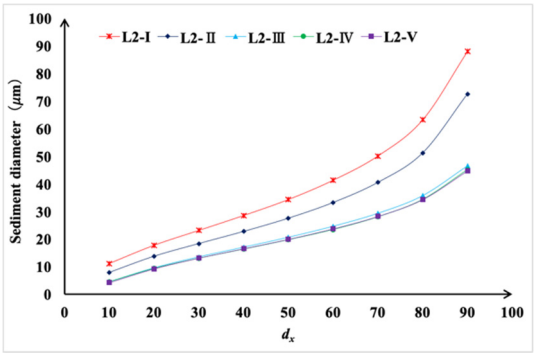

(**c**)

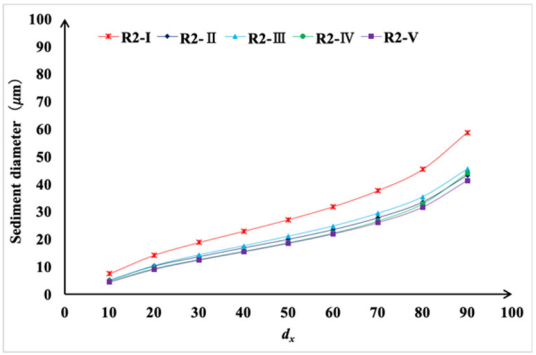

(**d**)

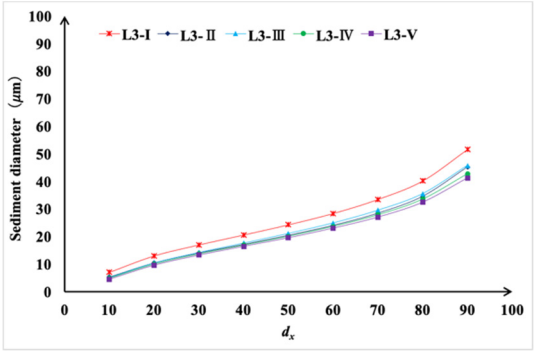

(**e**)

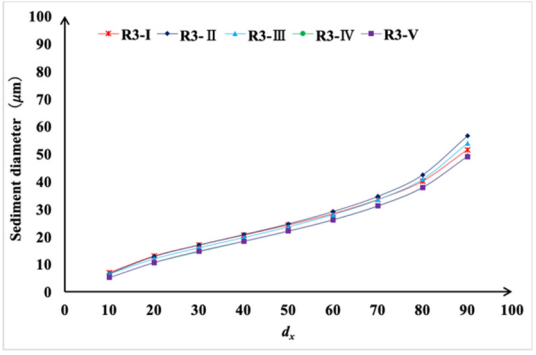

(**f**)

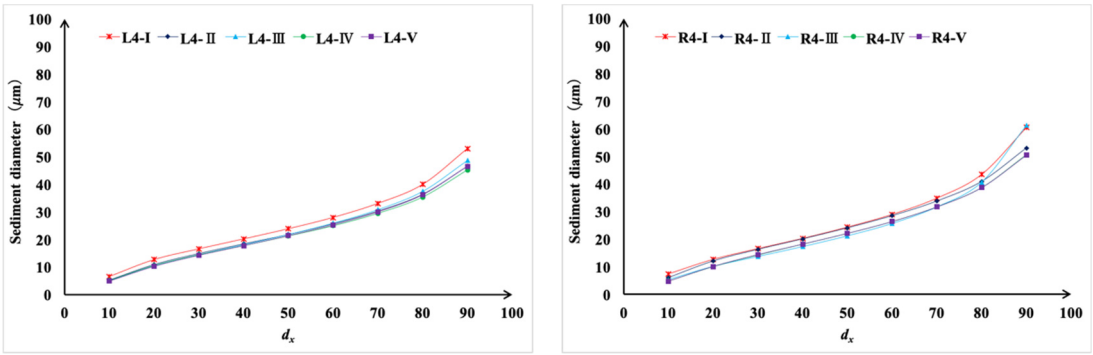

(**g**) (**h**)

Figure 10. Sediment size grading distribution at different locations in the settlement area with inclined tubes (ISA): (**a**) tube L1, (**b**) tube R1, (**c**) tube L2, (**d**) tube R2, (**e**) tube L3, (**f**) tube R3, (**g**) tube L4 and (**h**) tube R4. (The horizontal ordinate title d_x indicated the characteristic particle size.)

4. Discussion

How to remove fine sediment from water has been a concern among researchers. Many articles [34–36] have focused on the removal rate of different types of tanks, and most of the rates were between 37% and 62%. In this study, the fine sediment removal rate of the inclined-tube gravity sedimentation tank could reach 64.7–69.7%. The sediment particle size of *d90* at the outlet of the inclined tubes was about 40 μm. This would greatly reduce the clogging possibility of emitters in drip irrigation systems, as a study has shown that irrigation emitter blockage would increase sharply when the particle size is larger than 50 μm [37]. In order to deposit the fine sediment in the water as much as possible, the size of sedimentation tanks with a conventional structure was often very large. For example, the diameter of a circular-ring sedimentation tank used in Xinjiang, China was 30 m [38]. A circular sedimentation tank used in Thessaloniki, Greece had a volume of 2960 m^3 [7]. The water treatment efficiency per unit volume of the inclined-tube gravity sedimentation tank was found to be significantly higher than that of traditional tanks. It would significantly reduce the construction investment in tanks and the water treatment costs.

The inclined tubes significantly increased the removal rate of fine particles. Many studies have found that during the settling process, the sediment in inclined tubes was delaminated [39–41]; that is, the large sediment settled in the inclined tubes first, while the fine sediment settled later. This phenomenon could also be explained by Stokes' Law. The flow in the inclined tubes was laminar [32,42,43], so the terminal velocity of sediment particles was proportional to the square of the particle radius. Therefore, the larger the particle size was, the easier it would deposit on the inclined tubes wall. Due to the different settling speeds of sediment with different particle sizes in the flow of inclined tubes, the sediment particle size grading varied with the height of the tubes in this study. There have been few studies of the proper arrangement of inclined tubes height. Here, we found that the characteristic particle sizes of tube heights IV (70 cm) and V (90 cm) were not significantly different, indicating that the effective vertical working height of the inclined tubes should be 70–90 cm. The plate spacing and layout of the inclined plate had a great influence on the sediment settling velocity [25,29,30]. Similarly, the proper tube diameter and layout of the inclined tubes could greatly improve the sediment removal efficiency [32,33]. However, at present, there are few inclined tubes with a layout other than 60° in the market; more research works on arrangement parameters of inclined tubes need to be performed in the future by numerical simulation. The results of this paper can be used to validate the mathematical model of the numerical simulation.

Some structures in the inclined-tube gravity sedimentation tank were not conducive to the stable settling of fine sediment. The flow velocity from the water inlet was high, which not only washed away the sediment that had been deposited at the bottom of the FAA and made it re-suspend, reducing the settling efficiency of the tank, but also affected the structural stability of the tank bottom, which is not conducive to the long-term safe operation of the tank. This disadvantage could be

improved by reducing the flow velocity from the inlet and raising the inlet position. Moreover, the water flowing into the ISA from the gap between the baffle and the bottom of the tank resulted in the flow velocity increasing slightly and the sediment at the tank bottom being washed away; this result was also found in other research [44]. In addition, the suction effect of the overflow weir also negatively affected the stable settling of fine sediment. Different types of weirs proposed in many studies could inspire the optimization of the overflow weir structure used in this study [45–47].

5. Conclusions

Compared with the sedimentation tank with a conventional structure currently used in the Hetao irrigation district, the inclined-tube gravity sedimentation tank was much more efficient at fine sediment removal. A better understanding of the sediment movement in the tank was of great significance for further optimizing the structural parameters of the tank and improving the settling efficiency. Therefore, instruments such as a turbidimeter and a laser particle size analyzer were used here to measure the sediment concentration distribution and sediment size grading at different locations in the tank, as well as the deposited thickness of sediment at the bottom of the tank. The main conclusions of the research are as follows.

(1) The sediment concentration decreased rapidly in the front part of the SSA and the ISA. Large sediment mainly deposited in the FAA and the front part of the SSA, and the ISA had a great effect on fine sediment removal. The sediment removal rate of the inclined-tube gravity sedimentation tank could reach 64.7–69.7%, significantly higher than that of the sedimentation tank with a conventional structure (with a sediment removal rate of 20.7–32%).
(2) Except for some locations, the characteristic particle sizes at different locations on the tank bottom gradually decreased along the x direction. As for the particle size in the inclined tubes, it was larger in the lower part than in the upper part, and it was larger in the left tubes near the overflow weir than in the right tubes. The results showed that the effective vertical working height of the inclined tubes should be 70–90 cm, and the particle size of $d90$ at the outlet of the inclined tubes was significantly smaller than that in the test water source.
(3) The water inlet, baffle, and overflow weir would reduce the fine sediment removal and require further optimization.

The creativity of this study lies in the systematic measurement of the sediment concentration and the size grading at different locations in the tank, enhancing our understanding of the sedimentation characteristics in the inclined-tube gravity sedimentation tank. Further, the results of this paper can provide a technical basis for the structural parameter optimization of inclined-tube gravity sedimentation tanks and improvements of settling efficiency.

Author Contributions: Methodology, K.W. and P.Y.; investigation, K.W.; data curation, K.W. and S.R.; writing—original draft preparation, K.W.; writing—review and editing, K.W. and Y.L.; supervision, P.Y.; funding acquisition, P.Y. All authors have read and agreed to the published version of the manuscript.

Funding: This research was supported by the National Natural Science Foundation of China (51621061) and the Major Science and Technology Projects of Inner Mongolia (2014[117]). The funders had no role in the study design, data collection and analysis, decision to publish, or preparation of the manuscript.

Acknowledgments: We are deeply grateful to the editor and reviewers for their insightful and careful review.

Conflicts of Interest: The authors declare no conflict of interest.

References

1. Han, S.; Li, Y.; Xu, F.; Sun, D.; Feng, J.; Liu, Z.; Wu, R.; Wang, Z. Effect of lateral flushing on emitter clogging under drip irrigation with Yellow River water and a suitable method. *Irrig. Drain.* **2018**, *67*, 199–209.
2. Li, Q.; Song, P.; Zhou, B.; Xiao, Y.; Muhammad, T.; Liu, Z.; Zhou, H.; Li, Y. Mechanism of intermittent fluctuated water pressure on emitter clogging substances formation in drip irrigation system utilizing high sediment wate. *Agric. Water Manag.* **2019**, *215*, 16–24.
3. Zhou, H.; Li, Y.; Wang, Y.; Zhou, B.; Bhattarai, R. Composite fouling of drip emitters applying surface water

with high sand concentration: Dynamic variation and formation mechanism. *Agric. Water Manag.* **2019**, *215*, 25–43.
4. Bajcar, T.; Steinman, F.; Sirok, B.; Preseren, T. Sedimentation efficiency of two continuously operating circular settling tanks with different inlet- and outlet arrangements. *Chem. Eng. J.* **2011**, *178*, 217–224.
5. Bajcar, T.; Gosar, L.; Sirok, B.; Steinman, F.; Rak, G. Influence of flow field on sedimentation efficiency in a circular settling tank with peripheral inflow and central effluent. *Chem. Eng. Process. Process Intensif.* **2010**, *49*, 514–522.
6. Krebs, P. Success and shortcomings of clarifier modelling. *Water Sci. Technol.* **1995**, *31*, 181–191.
7. Goula, A.M.; Kostoglou, M.; Karapantsios, T.D.; Zouboulis, A.I. A CFD methodology for the design of sedimentation tanks in potable water treatment: Case study: The influence of a feed flow control baffle. *Chem. Eng. J.* **2008**, *140*, 110–121.
8. Tamayol, A.; Firoozabadi, B.; Ahmadi, G. Effects of Inlet Position and Baffle Configuration on Hydraulic Performance of Primary Settling Tanks. *J. Hydraul. Eng.* **2008**, *134*, 1004–1009.
9. Shahrokhi, M.; Rostami, F.; Said, M.A.M. Numerical modeling of baffle location effects on the flow pattern of primary sedimentation tanks. *Appl. Math. Model.* **2013**, *37*, 4486–4496.
10. Shahrokhi, M.; Rostami, F.; Said, M.A.M.; Yazdi, S.R.S.; Syafalni, S. Computational investigations of baffle configuration effects on the performance of primary sedimentation tanks. *Water Environ. J.* **2013**, *27*, 484–494.
11. Shahrokhi, M.; Rostami, F.; Said, M.A.M.; Yazdi, S.R.S.; Syafalni, S.; Abdullah, R. The effect of baffle angle on primary sedimentation tank efficiency. *Can. J. Civil Eng.* **2012**, *39*, 293–303.
12. Shahrokhi, M.; Rostami, F.; Said, M.A.M.; Yazdi, S.R.S.; Syafalni, S. The effect of number of baffles on the improvement efficiency of primary sedimentation tanks. *Appl. Math. Model.* **2012**, *36*, 3725–3735.
13. Csépai, L.; Kabelka, H. Practical testing of automatically controlled overflow weirs. *Water Res.* **1996**, *30*, 749–752.
14. Zong, Q.; Liu, H.; Tang, H.; Wu, J. Study of effect of spillway trough on spillway crest length of settling basin. *J. Sediment Res.* **2011**, 3, 67–72.
15. Hua, G.; Liu, H.; Tang, H.; Zong, Q.; Gao, X. Experimental study of effect on sediment deposition in the new-type rectangular settling tanks. *China Water Resour.* **2010**, 5, 8–10.
16. Zhang, Y.; Zhang, Y.; Chang, Z. An experimental study of hydraulic characteristics on automatic flushing desilting basin. *J. Irrig. Drain.* **2009**, 28, 78–82.
17. Wu, J.; Zong, Q.; Liu, H.; Liu, C. Experiment study of flow's adjusting with flow board in sediment basin. *J. Water Resour. Water Eng.* **2007**, *18*, 6–9.
18. Aldulaimi, S.M.S.;Racoviteanu, G. Performance of the tube settler clarification at different inclination angles and variable flow rate. *Mathematical Modelling in Civil Engineering.* **2018,** *14,* 13-25.
19. Culp, G.;Hansen, S.P.;Richardson, G. High-rate sedimentation in water treatment works. *Journal American Water Works Association.* **1968,** *60,* 681-698.
20. Fouad, H.A.;Elhefny, R.M.;Marei, A. Evaluating the use of tube settlers and lamella plates in Increasing the efficiency of sedimentation tanks. *Journal of Applied Life Sciences International.* **2016,** *7,* 1-8.
21. Fujisaki, K. Improvement of settling tank performance using inclined tube settlers. *Water Resources Management III.* **2005,** *80,* 475-484.
22. Gurjar, A.;Bhorkar, M. Performance study of tube settlers module. *International Journal of Engineering Research Applications of Mathematics.* **2017,** *07,* 52-55.
23. Hassan, M.S.;Hassan, A.H. The efficiency of using tube settlers technique in comparison with the conventional treatment in Mosul city water treatment. *Al Rafadain Engineering Journal.* **2009,** *19,* 26-34.
24. Yao, K.M. Design of high-rate settlers. *Journal of the Environmental Engineering Division.* **1973,** *99,* 621-637.
25. Sarkar, S.; Kamilya, D.; Mal, B. Effect of geometric and process variables on the performance of inclined plate settlers in treating aquacultural waste. *Water Res.* **2007**, *41*, 993–1000.
26. Salem, A.; Okoth, G.; Thöming, J. An approach to improve the separation of solid–liquid suspensions in inclined plate settlers: CFD simulation and experimental validation. *Water Res.* **2011**, *45*, 3541–3549.
27. Balwan, K.S.;Mujawar, A.;Karake, M. *To Study the Effect of Tube Settler on Clarification*. 2018;
28. T.Subramani;Thomas, S. Experiments on tube settler for the treatment of Fbw and optimization of plant operation for residual reduction. *International Journal of Engineering Research and Applications.* **2012,** *2,* 190-203.
29. Demïr, A. Determination of settling efficiency and optimum plate angle for plated settling tanks. *Water Res.*

1995, *29*, 611–616.
30. Abdolzadeh, M.; Mehrabian, M.; Goharrizi, A.S. Numerical study to predict the particle deposition under the influence of operating forces on a tilted surface in the turbulent flow. *Adv. Powder Technol.* **2011**, *22*, 405–415.
31. Bandrowski, J.; Hehlmann, J.; Merta, H.; Zioło, J. Studies of sedimentation in settlers with packing. *Chem. Eng. Process. Process. Intensif.* **1997**, *36*, 219–229.
32. Xie, M.; Shi, Z.; Liu, X. The motion and removal efficiency of particles in circular tube settlers. In Proceedings of the 2009 International Conference on Energy and Environment Technology, Guilin, Guangxi, China, 16–18 October 2009; Volume 1, pp. 437–440.
33. Ignjatović, L. Efficient (tube) settling tanks. *Water Sci. Technol.* **1991**, *24*, 223–228.
34. Casonato, M.; Gallerano, F. A finite difference self-adaptive mesh solution of flow in a sedimentation tank. *Int. J. Numer. Methods Fluids.* **1990**, *10*, 697–711.
35. Liu, X.; García, M.H. Computational fluid dynamics modeling for the design of large primary settling tanks. *J. Hydraul. Eng.* **2010**, *137*, 343–355.
36. Maruejouls, T.; Vanrolleghem, P.A.; Pelletier, G.; Lessard, P. A phenomenological retention tank model using settling velocity distributions. *Water Res.* **2012**, *46*, 6857–6867.
37. Niu, W.; Liu, L.; Chen, X. Influence of fine particle size and concentration on the clogging of labyrinth emitters. *Irrig. Sci.* **2013**, *31*, 545–555.
38. Zhang, J.; Shi, K.; Gao, Y.; Wang, J. Turbid water desilting characteristics of circular-ring desilting and sediment ejection basin. *Trans. Chin. Soc. Agric Eng.* **2014**, *30*, 86–93.
39. Doroodchi, E.; Fletcher, D.F.; Galvin, K.P. Influence of inclined plates on the expansion behaviour of particulate suspensions in a liquid fluidised bed. *Chem. Eng. Sci.* **2004**, *59*, 3559–3567.
40. Laux, H.;Ytrehus, T. Computer simulation and experiments on two-phase flow in an inclined sedimentation vessel. *Powder Technology.* **1997,** *94,* 35-49.
41. Schlieper, L.; Chatterjee, M.; Henschke, M.; Pfennig, A. Liquid–liquid phase separation in gravity settler with inclined plates. *AIChE J.* **2004**, *50*, 802–811.
42. Clay Mcmichael, F. Sedimentation in inclined tubes And its application for the design of high rate sedimentation devices. *Journal of hydraulic Research.* **1972,** *10,* 59-75.
43. Yao, K. Theoretical study of high-rate sedimentation. *Journal(Water Pollution Control Federation).* **1970,** 218-228.
44. Zhou, S.; McCorquodale, J.A. Modeling of rectangular settling tanks. *J. Hydraul. Eng.* **1992**, *118*, 1391–1405.
45. Lv, X.; Zou, Q.; Reeve, D. Numerical simulation of overflow at vertical weirs using a hybrid level set/VOF method. *Adv. Water Resour.* **2011**, *34*, 1320–1334.
46. Chen, Y.; Fu, Z.; Chen, Q.; Cui, Z. Discharge Coefficient of Rectangular Short-Crested Weir with Varying Slope Coefficients. *Water* **2018**, *10*, 204.
47. Khode, B.; Tembhurkar, A.; Porey, P.; Ingle, R. Experimental studies on flow over labyrinth weir. *J. Irrig. Drain. Eng.* **2011**, *138*, 548–552.